nature genetics

Gain-of-function mutations in *IFIH1* cause a spectrum of human disease phenotypes associated with upregulated type I interferon signaling

Gillian I Rice[1,46], Yoandris del Toro Duany[2,3,46], Emma M Jenkinson[1], Gabriella M A Forte[1], Beverley H Anderson[1], Giada Ariaudo[4,5], Brigitte Bader-Meunier[6], Eileen M Baildam[7], Roberta Battini[8], Michael W Beresford[7,9], Manuela Casarano[8], Mondher Chouchane[10], Rolando Cimaz[11], Abigail E Collins[12], Nuno J V Cordeiro[13], Russell C Dale[14], Joyce E Davidson[15], Liesbeth De Waele[16], Isabelle Desguerre[17], Laurence Faivre[18], Elisa Fazzi[19], Bertrand Isidor[20,21], Lieven Lagae[16], Andrew R Latchman[22], Pierre Lebon[23], Chumei Li[24], John H Livingston[25], Charles M Lourenço[26], Maria Margherita Mancardi[27], Alice Masurel-Paulet[18], Iain B McInnes[28], Manoj P Menezes[29], Cyril Mignot[30], James O'Sullivan[1], Simona Orcesi[4], Paolo P Picco[31], Enrica Riva[32], Robert A Robinson[33], Diana Rodriguez[34–36], Elisabetta Salvatici[32], Christiaan Scott[37], Marta Szybowska[24], John L Tolmie[38], Adeline Vanderver[39], Catherine Vanhulle[40], Jose Pedro Vieira[41], Kate Webb[37], Robyn N Whitney[42], Simon G Williams[1], Lynne A Wolfe[43], Sameer M Zuberi[44,45], Sun Hur[2,3,47] & Yanick J Crow[1,47]

The type I interferon system is integral to human antiviral immunity. However, inappropriate stimulation or defective negative regulation of this system can lead to inflammatory disease. We sought to determine the molecular basis of genetically uncharacterized cases of the type I interferonopathy Aicardi-Goutières syndrome and of other undefined neurological and immunological phenotypes also demonstrating an upregulated type I interferon response. We found that heterozygous mutations in the cytosolic double-stranded RNA receptor gene *IFIH1* (also called *MDA5*) cause a spectrum of neuroimmunological features consistently associated with an enhanced interferon state. Cellular and biochemical assays indicate that these mutations confer gain of function such that mutant IFIH1 binds RNA more avidly, leading to increased baseline and ligand-induced interferon signaling. Our results demonstrate that aberrant sensing of nucleic acids can cause immune upregulation.

Ion Gresser and colleagues first drew attention to the possibility that inappropriate exposure to type I interferon might be detrimental in mammals[1–3]. More recently, it has been proposed that mendelian disorders associated with an upregulation of type I interferon represent a distinct set of inborn errors of immunity, resulting from either inappropriate stimulation or defective negative regulation of the type I interferon response pathway[4].

Aicardi-Goutières syndrome (AGS; MIM 225750) is an inflammatory disease particularly affecting the brain and skin, occurring as a result of mutations in any of the genes encoding the DNA exonuclease TREX1 (ref. 5), the three non-allelic components of the RNase H2 endonuclease complex[6], the deoxynucleoside triphosphate triphosphohydrolase SAMHD1 (ref. 7) and the double-stranded RNA (dsRNA) editing enzyme ADAR1 (ref. 8). Some individuals with AGS do not harbor mutations in any of these six genes. AGS cases consistently demonstrate higher expression of genes induced by type I interferon, a so-called interferon signature[9]. A similar upregulation of interferon-induced transcripts is seen in the immuno-osseous dysplasia spondyloenchondromatosis (SPENCD)[10].

To identify further monogenic type I interferonopathies, we set out to determine the molecular basis of genetically uncharacterized cases of AGS and of other undefined neurological and immunological features also demonstrating an upregulated type I interferon response. Here we show that gain-of-function mutations in *IFIH1* result in a range of human disease phenotypes in which induction of type I interferon signaling is likely central to pathogenesis.

We undertook whole-exome sequencing (**Supplementary Table 1**) in three individuals (F102, F163 and F259) with a clinical diagnosis of AGS, based on neuroradiological criteria and upregulation of cerebrospinal fluid interferon activity and/or interferon-stimulated gene (ISG) expression in peripheral blood (**Supplementary Table 2**), all of whom screened negative for mutations in *TREX1*, *RNASEH2A*, *RNASEH2B*, *RNASEH2C*, *SAMHD1* and *ADAR*. Having excluded common polymorphisms listed in publically available databases, we noted that all three cases carried a single rare variant (resulting in p.Arg720Gln in F102 and p.Arg779His in both F163 and F259; **Table 1**) in *IFIH1*, which encodes a cytoplasmic helicase that mediates the

A full list of affiliations appears at the end of the paper.

Received 1 January; accepted 5 March; published online 30 March 2014; doi:10.1038/ng.2933

induction of an interferon response to viral RNA[11]. We then screened *IFIH1* in other individuals negative for mutations in *TREX1*, *RNASEH2A*, *RNASEH2B*, *RNASEH2C*, *SAMHD1* and *ADAR* with a phenotype indicative of AGS and in individuals with a variety of neuroimmunological features in whom we had recorded the presence of an interferon signature in peripheral blood in the absence of apparent infection (**Supplementary Tables 2** and **3**). In this way, we identified a further five probands each heterozygous for a rare *IFIH1* variant (resulting in p.Arg337Gly in F237, p.Arg779Cys in F376, p.Gly495Arg in F524, p.Asp393Val in F626 and p.Arg720Gln in F647). In total, we observed six rare variants in eight probands, with two pairs of unrelated probands each sharing the same substitution (p.Arg720Gln and p.Arg779His; **Fig. 1** and **Supplementary Fig. 1**). All mutation-positive probands were born to non-consanguineous parents.

Table 1 Ancestry and sequence alterations in *IFIH1* mutation–positive families

Family	Ancestry	Inheritance	Nucleotide alteration	Exon	Amino acid alteration	Domain	EVS allele frequency
F102	European Italian	*De novo*	c.2159G>A	11	p.Arg720Gln	Hel2	0/13,006
F163	European French	*De novo*	c.2336G>A	12	p.Arg779His	Hel2	0/13,006
F237	European American	*De novo*	c.1009A>G	5	p.Arg337Gly	Hel1	0/13,006
F259	European Italian	Inherited[a]	c.2336G>A	12	p.Arg779His	Hel2	0/13,006
F376	European British	NA	c.2335C>T	12	p.Arg779Cys	Hel2	0/13,006
F524	European British	*De novo*[b]	c.1483G>A	7	p.Gly495Arg	Hel1	0/13,006
F626	European Italian	*De novo*	c.1178A>T	6	p.Asp393Val	Hel1	0/13,006
F647	Mixed European, Irish and Ukrainian	*De novo*	c.2159G>A	11	p.Arg720Gln	Hel2	0/13,006

NA, not available; EVS, Exome Variant Server (see URLs).
[a]The mutation in the affected child was inherited from the mutation-positive clinically asymptomatic father. The proband's paternal grandmother also carries the mutation and is clinically asymptomatic. All three mutation-positive individuals demonstrate a robust interferon signature. [b]The mutation occurred *de novo* in an affected male, who then transmitted the mutation to his affected daughter.

The identified variants of interest were confirmed by Sanger sequencing and were considered likely pathogenic on the basis of species conservation (**Supplementary Figs. 2** and **3**), the output of pathogenicity prediction packages (**Supplementary Table 4**) and absence from the National Heart, Lung, and Blood Institute (NHLBI) Exome Sequencing Project (ESP) database of more than 13,000 control alleles and an in-house collection of >300 exomes. Parental samples were available for seven of the eight probands. For five of these seven, the variant was not present in either parent, although genotyping of microsatellite markers was consistent with stated paternity and maternity, indicating that the mutations had arisen *de novo* (**Supplementary Table 5**). In the remaining two cases (F259_1 and F524_1), the variant detected in the proband had been paternally inherited (**Supplementary Fig. 1**). In family F259, the variant had been transmitted by the proband's paternal grandmother (F259_3) to her son (F259_2), and, in family F524, the mutation was shown to have occurred *de novo* in the father (F524_2).

The majority of probands positive for mutation in *IFIH1* (F102, F163, F259_1, F376 and F647) demonstrated clinical characteristics typical of neonatal AGS (**Supplementary Table 2** and **Supplementary Note**). In contrast, two cases (F237 and F626) were developmentally normal until the second year of life, at which point they experienced rapid neuroregression. Of particular note, both affected individuals in family F524 (F524_1 and F524_2) presented a distinct phenotype of dominantly inherited spastic paraparesis. The finding of normal neuroimaging in F524_2 at the age of 29 years suggests that further cases with unexplained spasticity might harbor mutations in *IFIH1* or other AGS-related genes.

To define the relationship between *IFIH1* mutation status and interferon induction *in vivo*, we tested for an interferon signature in subjects positive for *IFIH1* mutation and in their mutation-negative relatives. Samples were available from five families (F237, F259, F524, F626 and F647). All 8 mutation-positive individuals assayed, over a total of 22 data points, demonstrated robust upregulation of ISG expression (median relative quantification (RQ) = 17.43, interquartile range (IQR) = 12.27–25.77) compared with 12 family members negative for *IFIH1* mutation assayed on 17 occasions (median RQ = 0.89, IQR = 0.52–1.12) and a previously standardized set of 29 control individuals (median RQ = 0.93, IQR = 0.57–1.30; **Fig. 2** and **Supplementary Fig. 4**). Where measured serially, positivity for an interferon signature was sustained over time (for example, subject F524_2 was assayed on five occasions over an 18-month period).

IFIH1 (interferon induced with helicase C domain 1), also known as MDA5 (melanoma differentiation-associated protein 5), is a 1,025-residue cytoplasmic viral RNA receptor. IFIH1 belongs to the RIG-I–like family of cytoplasmic DExD/H-box RNA receptors and

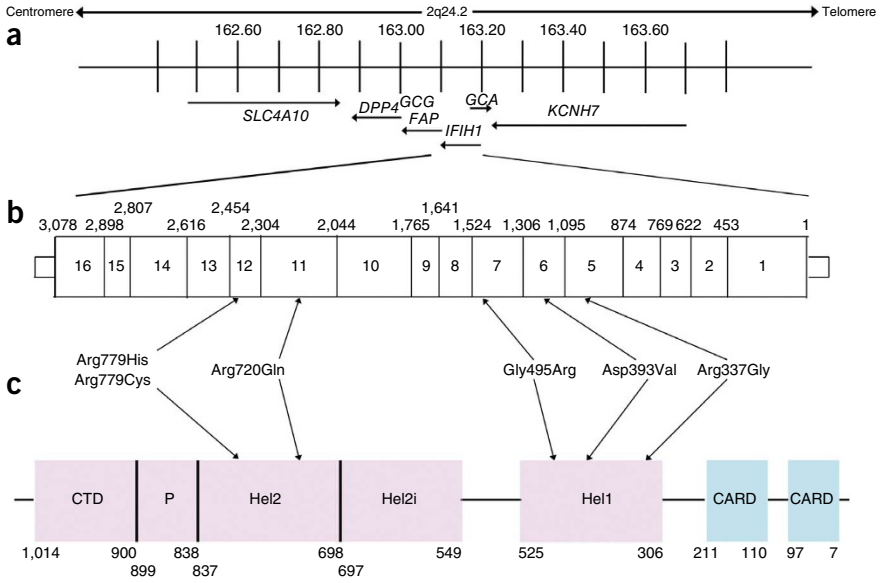

Figure 1 Schematic of the human *IFIH1* gene. (**a**) *IFIH1* spans 51,624 bp of genomic sequence on chromosome 2q24.2 (163,123,589–163,175,213). Neighboring genes are also shown. (**b**) Positions of identified variants within the genomic sequence of *IFIH1*. Exons are numbered within the boxes. Numbers given above the gene indicate the positions of exon boundaries using cDNA numbering. (**c**) Schematic showing the positions of protein domains and their amino acid boundaries within the IFIH1 1,025-residue protein. CARD, caspase activation recruitment domain; Hel, helicase domain, where Hel1 and Hel2 are the two conserved core helicase domains and Hel2i is an insertion domain that is conserved in the RIG-I–like helicase family; P, pincer or bridge region connecting Hel2 to the C-terminal domain (CTD) involved in binding dsRNA.

activates type I interferon signaling through an adaptor molecule, MAVS (mitochondrial antiviral signaling protein). IFIH1 consists of N-terminal tandem caspase activation recruitment domains (2CARD) involved in activating MAVS, a central helicase domain responsible for RNA binding and RNA-dependent ATP hydrolysis, and a C-terminal domain serving as an additional RNA-binding domain (**Fig. 1**). IFIH1 uses long viral dsRNA as a platform to cooperatively assemble a core filament, which in turn promotes stochastic assembly

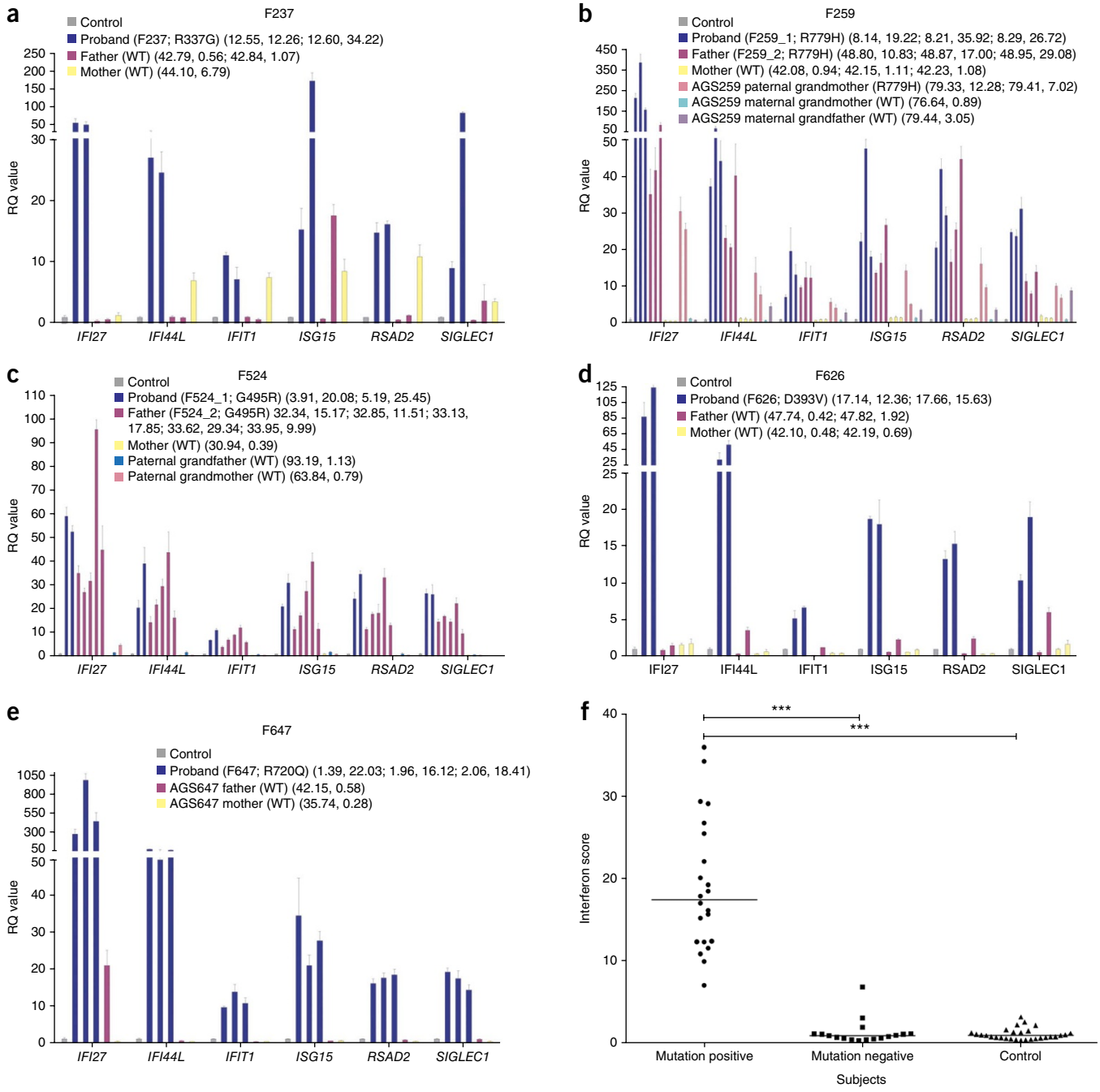

Figure 2 Quantitative RT-PCR (qPCR) of a panel of six ISGs in whole blood measured in *IFIH1* mutation–positive probands and mutation-negative relatives and interferon scores in mutation-positive individuals, mutation-negative relatives and controls. (**a**–**e**) Bar graphs showing relative quantification (RQ) values for a panel of 6 ISGs (*IFI27*, *IFI44L*, *IFIT1*, *ISG15*, *RSAD2*, *SIGLEC1*) measured in whole blood in 5 families with AGS compared to the combined results of 29 healthy controls: results are shown for F237 (**a**), F259 (**b**), F524 (**c**), F626 (**d**) and F647 (**e**). The RQ value is equal to $2^{-\Delta\Delta Ct}$, with $-\Delta\Delta C_t \pm$ s.d. (i.e., normalized fold change relative to a calibrator). Each value is derived from three technical replicates. Family or case numbers followed by mutation status are given in the first set of parentheses. Numbers in the second set of parentheses refer to decimalized age (in years) at sampling followed by the interferon score calculated from the median fold change in the RQ value for the panel of six ISGs. Colors denote individuals, with repeat samples (biological replicates) denoted by different bars of the same color. WT, wild type. (**f**) Interferon score in all affected individuals, relatives and controls calculated from the median fold change in RQ value for a panel of six ISGs. For participants with repeat samples, all measurements are shown. Black horizontal bars show the median interferon scores in mutation-positive, mutation-negative and control individuals. Data were analyzed by one-way ANOVA using the Bonferroni multiple-comparison test (***$P < 0.0001$).

of the 2CARD oligomers for signaling to MAVS[12–14]. The IFIH1 filament undergoes end disassembly upon ATP hydrolysis[13], thereby regulating the stability of the filament in a dsRNA length–dependent manner, in a potential mechanism to suppress aberrant signal activation in response to short (<~0.5-kb) cellular dsRNA.

To understand the pathogenicity of the *IFIH1* mutations observed, we investigated the interferon β (IFN-β) reporter stimulatory activity of wild-type and mutant IFIH1 in human embryonic kidney (HEK) 293T cells. HEK 293T cells express low levels of endogenous viral RNA receptors, including IFIH1, as evidenced by low interferon production upon stimulation with dsRNA (**Fig. 3a**), allowing comparison of the signaling activity of ectopically expressed receptors. As expected, signaling of wild-type IFIH1 was induced only upon addition of the long (>1-kb) dsRNA analog polyinosinic:polycytidylic acid (poly I:C)

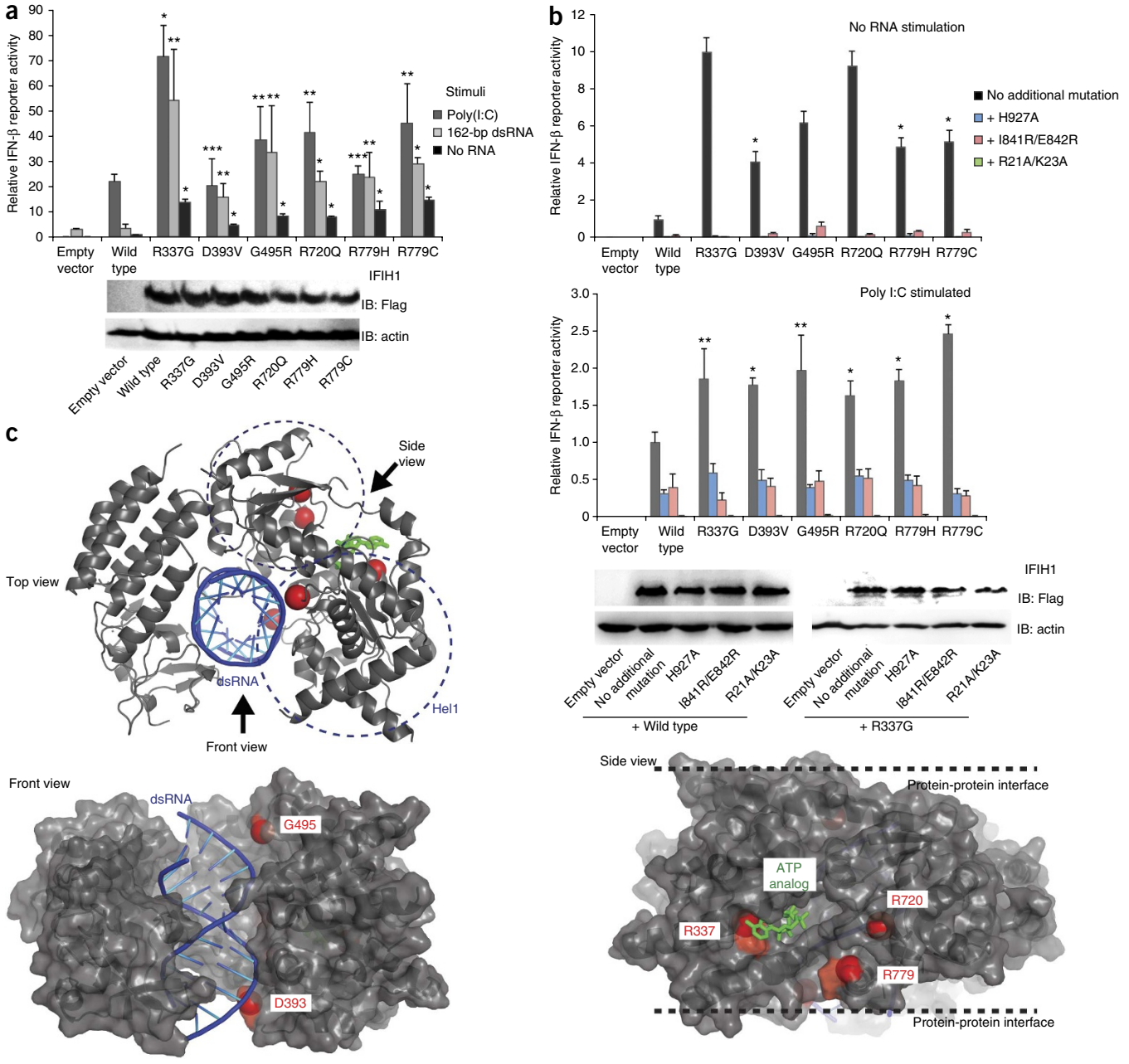

Figure 3 IFIH1 mutants activate the interferon signaling pathway more efficiently than wild-type IFIH1. (**a**) IFN-β reporter activity (mean ± s.d., $n = 3$ biological replicates) of Flag-tagged wild-type and mutant IFIH1 with and without stimulation with poly I:C or 162-bp dsRNA in HEK 293T cells. The results are representative of three independent experiments. $^{*}P < 0.005$, $^{**}P < 0.05$, $^{***}P < 0.5$ (one-tailed, unpaired *t* test, compared with wild-type values). Shown below are protein blots for Flag and actin indicating the expression levels of IFIH1 and the internal control (actin), respectively. IB, immunoblot. (**b**) IFN-β reporter activity (mean ± s.d., $n = 3$ biological replicates) of mutant IFIH1 with and without additional substitutions (His927Ala, Ile841Arg/Glu842Arg or Arg21Ala/Lys23Ala) that disrupt RNA binding, filament formation or 2CARD signal activation by IFIH1. Reporter activity was measured in the absence (top) or presence (bottom) of poly I:C stimulation in HEK 293T cells. IFIH1 expression constructs (10 and 20 ng) were used with and without poly I:C, respectively. The results are representative of three independent experiments. $^{*}P < 0.005$, $^{**}P < 0.05$ (one-tailed, unpaired *t* test). Below are protein blots showing the expression levels of wild-type and Arg337Gly IFIH1 with and without His927Ala, Ile841Arg/Glu842Arg and Arg21Ala/Lys23Ala. (**c**) Mapping of the altered residues (red spheres) onto the structure of IFIH1Δ2CARD (gray) bound by dsRNA (blue) and ATP analog (green) (PDB 4GL2).

and not by short, 162-bp dsRNA (**Fig. 3a**). Minimal activity was seen in the absence of exogenous RNA (**Fig. 3a**). As with wild-type IFIH1, all six IFIH1 mutants displayed robust signaling in response to poly I:C (**Fig. 3a**). Additionally, these mutants exhibited a marked induction of interferon signaling in response to 162-bp dsRNA (**Fig. 3a**) and demonstrated ~4- to 10-fold higher levels of basal signaling activity even in the absence of exogenous ligand (**Fig. 3b**). As with poly I:C–induced signaling of wild-type IFIH1, the basal and induced signaling activities of the six mutants were significantly ($P < 0.005$) diminished upon the introduction of additional alterations in the RNA-binding site (p.His927Ala), the filament protein-protein interface (p.Ile841Arg and p.Glu842Arg) and 2CARD (p.Arg21Ala and p.Lys23Ala) (**Fig. 3b**)[13], suggesting that the basal signaling activity of these mutants is induced by as-yet-undefined endogenous dsRNA.

Mapping of the altered residues onto the crystal structure of the 2CARD deletion construct (Δ2CARD)[14] showed that these residues were located on the surface of the RNA-binding and ATP-binding sites in the Hel1 and Hel2 helicase domains (**Fig. 3c**). In particular, Arg337 was in direct contact with the adenine base of ATP, stabilizing the IFIH1-ATP interaction. Substitution of Arg337 by glycine could diminish the ATP binding and hydrolysis activities of IFIH1. Asp393 and Gly495 were located within the contact distance of bound RNA. Removal of the negatively charged Asp393 residue (by p.Asp393Val) and incorporation of positively charged Arg495 (by p.Gly495Arg) near the RNA phosphate backbone could increase the intrinsic affinity of IFIH1 for dsRNA. Arg720 and Arg779 were located near the ATP-binding site but were also in proximity to the protein-protein interface in the filament (**Fig. 3c**). The location of the altered residues in or near the RNA-binding and ATP-binding sites or the filament interface led us to hypothesize that the observed mutations might enhance the stability of the IFIH1 filament by increasing the intrinsic affinity between IFIH1 and dsRNA or between IFIH1 molecules in the filament or by decreasing the efficiency of ATP hydrolysis and, thus, filament disassembly rate.

To examine these possibilities, we purified individual mutants of the Δ2CARD construct, which is both necessary and sufficient for dsRNA binding, filament formation and ATP hydrolysis[14]. As previously described[12,13], electrophoretic mobility shift assays (EMSAs) showed that wild-type Δ2CARD cooperatively binds dsRNA in the absence of ATP but accumulates complexes of intermediate size upon

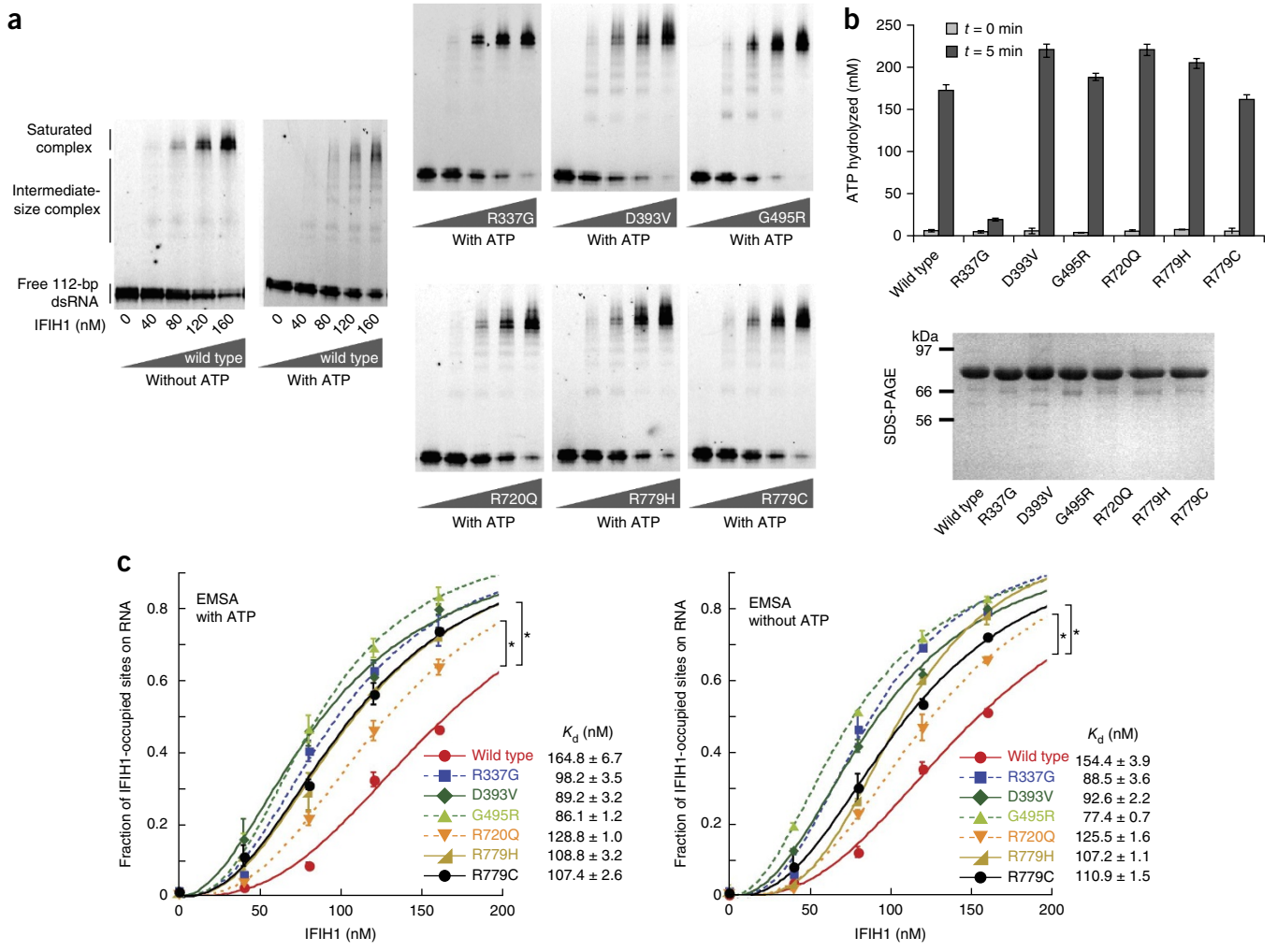

Figure 4 IFIH1 mutants form filaments. (**a**) EMSA of purified wild-type and mutant IFIH1 with 112-bp dsRNA. Gel images are representative of three independent experiments. (**b**) ATP hydrolysis activity (mean ± s.d., $n = 3$ biological replicates) of wild-type and mutant IFIH1. Shown below is SDS-PAGE analysis (Coomassie stain) of the purified wild-type and mutant IFIH1 used in **Figure 3**. (**c**) Fraction of IFIH1-occupied sites on 112-bp dsRNA, measured from three independent EMSAs performed in the presence and absence of ATP. $^*P < 0.0002$ (one-tailed, unpaired t test), calculated using the values at 160 nM IFIH1. Bound fraction was calculated as described[12] and fitted with the Hill equation[29]. Dissociation constants (K_d) obtained from curve fitting are shown.

the addition of ATP (**Fig. 4a**). This observation is consistent with our previous finding that ATP hydrolysis induces rapid cycles of filament disassembly and reassembly[12,13]. Interestingly, the population of these intermediate-size complexes was markedly diminished with all six mutants, in particular with Arg337Gly, showing few or no such complexes. Measurement of ATP hydrolysis activity demonstrated that, with the exception of Arg337Gly, all the mutants hydrolyzed ATP as well as wild-type protein (**Fig. 4b**). This finding rules out a lack of ATP hydrolysis as a reason for these five mutants to assemble filaments more cooperatively than wild-type protein. Quantitative analysis of the RNA-bound IFIH1 fraction from EMSAs showed that all six mutants bound RNA more efficiently than wild-type IFIH1, both in the presence and absence of cellular levels (2 mM) of ATP (**Fig. 4c**). These results suggest that ATP-independent mechanisms, i.e., tighter RNA binding and/or more stable protein-protein interaction, are likely responsible for the observed stability of the IFIH1 filament *in vitro* (**Fig. 4a**) and for higher signaling activity in cells (**Fig. 3a**,**b**).

Here we describe 6 heterozygous *IFIH1* mutations in a total of 11 individuals from 8 families, where mutation-positive status is consistently associated with an induction of type I interferon activity. The finding of *de novo* mutations in six families and the dominant inheritance of a clinical (F524) and/or biochemical (F524 and F259) phenotype in two families strongly suggest that these mutations are pathogenic in the heterozygous state and that *IFIH1* represents a seventh gene in which mutations are associated with the AGS phenotype. Although AGS is most typically inherited as an autosomal recessive trait, rare examples due to dominant mutations in *TREX1* (ref. 15) and *ADAR*[8] have been described.

A striking feature in family F259 was the marked clinical discordance between the affected child (F259_1) and his clinically asymptomatic, mutation-positive father (R259_2) and paternal grandmother (F259_3) (**Supplementary Fig. 1**), despite upregulation of type I interferon signaling in all three individuals (**Fig. 2**). Thus, mutation positivity and positivity for an interferon signature are not necessarily sufficient to develop an overt clinical phenotype. Notably, the same mutation (resulting in p.Arg779His), dominantly transmitted across three generations in family F259, was found to occur *de novo* in the proband of family F163. We and others have described both severe neurological disease and non-penetrance or age-dependent penetrance in the context of a recurrent mutation in *ADAR* (resulting in a p.Gly1007Arg substitution), which can also be dominantly inherited or occur as a new mutation[16–18]. Such clinical variability might be explained by modifying genetic factors or differential exposure to pathogens.

Most individuals with the autoimmune disease systemic lupus erythematosus (SLE) demonstrate an interferon signature[19,20], and polymorphisms in *IFIH1* confer increased risk of developing SLE[21]. In keeping with these observations, two cases in our cohort (F376 and F524_1) experienced substantial immunological disturbance consistent with lupus. The finding that the majority of *IFIH1* mutation–positive individuals had no overt lupus phenotype again suggests the importance of modifying genetic or environmental factors and is concordant with a multicopy *Ifih1* transgenic mouse line demonstrating chronically elevated levels of type I interferon, insufficient by themselves to initiate autoimmunity[22].

Nejentsev *et al.*[23] described two canonical splice-site variants—a nonsense variant and a missense substitution—in *IFIH1* as protective against type 1 diabetes (T1D) (**Supplementary Table 6**). They postulated that these presumed loss-of-function alleles attenuate the immune response to enterovirus, a factor implicated in the pathogenesis of T1D. Unlike the variants reported in that study, all of the mutations described here are missense substitutions conferring a gain of function, and none have been documented in the NHLBI ESP database. Thus far, none of our *IFIH1* mutation–positive cases have developed T1D.

Studies of the AGS-related proteins TREX1, the RNase H2 complex, SAMHD1 and ADAR1 suggest that an inappropriate accumulation of self-derived nucleic acids can induce type I interferon signaling[24,25]. The finding of *IFIH1* mutations in a similar context implicates aberrant sensing of nucleic acids as a cause of immune upregulation. The observation of enhanced baseline and ligand-induced type I interferon signaling by all six mutant alleles is consistent with our observation of increased interferon activity and/or ISG transcript levels in every mutation-positive individual tested. It is also consistent with our biochemical analyses showing that the mutants bind dsRNA more avidly and tightly than wild-type protein, albeit to a varying degree, indicating that even small differences in binding can result in a different biological phenotype. These mutations provide new insights into the function of IFIH1, which might be useful in designing therapies to potentiate host antiviral innate immunity.

The dependence of mutant basal signaling activity on dsRNA binding and filament formation suggests the presence of as-yet-undefined endogenous dsRNA capable of stimulating mutant but not wild-type receptor. In light of observed clinical non-penetrance and the rapid onset of neurological regression in the second year of life in two cases, we cannot dismiss the possibility that exogenous viral-derived RNA[26] also has a role in the disease process. We note the description of an *N*-ethyl-*N*-nitrosourea (ENU)-induced *Ifih1* missense mutation in a mouse model demonstrating upregulated interferon signaling and an autoimmune phenotype[27]. In contrast to the mutants that we describe, signaling by this mutant was ligand independent.

We have previously reported an interferon signature as a reliable biomarker for AGS[9] and SPENCD[10]. The current study further emphasizes the value of searching for an interferon signature as a screening tool to identify other type I interferonopathies[4]. The recognition of such diseases is not just of academic interest, as defining a disturbance of type I interferon as primary to the pathogenesis of an aberrant phenotype suggests the possibility of anti-interferon and anti-inflammatory therapies[28].

URLs. UCSC Human Genome Browser, http://genome.ucsc.edu/; Ensembl, http://www.ensembl.org/; dbSNP, http://www.ncbi.nlm.nih.gov/projects/SNP/; Exome Variant Server, NHLBI Exome Sequencing Project (ESP) (accessed 17 October 2013), http://snp.gs.washington.edu/EVS/; PolyPhen-2, http://genetics.bwh.harvard.edu/pph2/; SIFT, http://sift.jcvi.org/www/SIFT_enst_submit.html; MutationTaster, http://www.mutationtaster.org/; Clustal Omega, https://www.ebi.ac.uk/Tools/msa/clustalo/; Protein Data Bank (PDB), http://www.pdb.org/; Alamut, http://www.interactive-biosoftware.com/; GraphPad, http://www.graphpad.com/.

METHODS

Methods and any associated references are available in the online version of the paper.

Note: Any Supplementary Information and Source Data files are available in the online version of the paper.

ACKNOWLEDGMENTS

We sincerely thank the participating families for the use of genetic samples and clinical information and all clinicians who contributed samples and data not included in this manuscript. We thank D. Chase for proofreading the manuscript. We thank G. Notarangelo for helpful discussion. Y.d.T.D. holds a Novartis Foundation postdoctoral fellowship. S.H. holds a Pew scholarship and Career Development award from Boston Children's Hospital. Y.J.C. acknowledges the

Manchester Biomedical Research Centre, Manchester Academic Health Sciences Centre, the Greater Manchester Comprehensive Local Research Network, the Great Ormond Street Hospital Children's Charity, the European Union's Seventh Framework Programme (FP7/2007-2013) under grant agreement 241779 and the European Research Council (GA 309449). The authors would like to thank the NHLBI GO ESP and its ongoing studies, which produced and provided exome variant calls for comparison: the Lung GO Sequencing Project (HL-102923), the Women's Health Initiative (WHI) Sequencing Project (HL-102924), the Broad GO Sequencing Project (HL-102925), the Seattle GO Sequencing Project (HL-102926) and the Heart GO Sequencing Project (HL-103010).

AUTHOR CONTRIBUTIONS

B.H.A., J.O. and S.G.W. performed exome sequencing. E.M.J., G.I.R. and Y.J.C. performed exome data analysis. G.I.R. performed quantitative PCR analysis and Sanger sequencing with assistance from E.M.J. and G.M.A.F. G.M.A.F. and B.H.A. performed genotyping analysis with assistance from G.I.R. Y.d.T.D. performed IFIH1 protein studies. S.H. performed modeling studies. Y.J.C. and S.H. designed and supervised the project and wrote the manuscript, with support from G.I.R. G.A., B.B.-M., E.M.B., R.B., M.W.B., M. Casarano, M. Chouchane, R.C., A.E.C., N.J.V.C., R.C.D., J.E.D., L.D.W., I.D., L.F., E.F., B.I., L.L., A.R.L., P.L., C.L., J.H.L., C.M.L., M.M.M., A.M.-P., I.B.M., M.P.M., C.M., S.O., P.P.P., E.R., R.A.R., D.R., E.S., C.S., M.S., J.L.T., A.V., C.V., J.P.V., K.W., R.N.W., L.A.W. and S.M.Z. identified affected individuals or assisted with related clinical and laboratory studies.

COMPETING FINANCIAL INTERESTS

The authors declare no competing financial interests.

1. Gresser, I., Tovey, M.G., Maury, C. & Chouroulinkov, I. Lethality of interferon preparations for newborn mice. *Nature* **258**, 76–78 (1975).
2. Gresser, I. *et al.* Progressive glomerulonephritis in mice treated with interferon preparations at birth. *Nature* **263**, 420–422 (1976).
3. Gresser, I. *et al.* Interferon-induced disease in mice and rats. *Ann. NY Acad. Sci.* **350**, 12–20 (1980).
4. Crow, Y.J. Type I interferonopathies: a novel set of inborn errors of immunity. *Ann. NY Acad. Sci.* **1238**, 91–98 (2011).
5. Crow, Y.J. *et al.* Mutations in the gene encoding the 3′-5′ DNA exonuclease TREX1 cause Aicardi-Goutières syndrome at the *AGS1* locus. *Nat. Genet.* **38**, 917–920 (2006).
6. Crow, Y.J. *et al.* Mutations in genes encoding ribonuclease H2 subunits cause Aicardi-Goutières syndrome and mimic congenital viral brain infection. *Nat. Genet.* **38**, 910–916 (2006).
7. Rice, G.I. *et al.* Mutations involved in Aicardi-Goutières syndrome implicate SAMHD1 as regulator of the innate immune response. *Nat. Genet.* **41**, 829–832 (2009).
8. Rice, G.I. *et al.* Mutations in *ADAR1* cause Aicardi-Goutières syndrome associated with a type I interferon signature. *Nat. Genet.* **44**, 1243–1248 (2012).
9. Rice, G.I. *et al.* Assessment of interferon-related biomarkers in Aicardi-Goutières syndrome associated with mutations in *TREX1*, *RNASEH2A*, *RNASEH2B*, *RNASEH2C*, *SAMHD1*, and *ADAR*: a case-control study. *Lancet Neurol.* **12**, 1159–1169 (2013).
10. Briggs, T.A. *et al.* Tartrate-resistant acid phosphatase deficiency causes a bone dysplasia with autoimmunity and a type I interferon expression signature. *Nat. Genet.* **43**, 127–131 (2011).
11. Goubau, D., Deddouche, S. & Reis, E.S.C. Cytosolic sensing of viruses. *Immunity* **38**, 855–869 (2013).
12. Peisley, A. *et al.* Cooperative assembly and dynamic disassembly of MDA5 filaments for viral dsRNA recognition. *Proc. Natl. Acad. Sci. USA* **108**, 21010–21015 (2011).
13. Peisley, A. *et al.* Kinetic mechanism for viral dsRNA length discrimination by MDA5 filaments. *Proc. Natl. Acad. Sci. USA* **109**, E3340–E3349 (2012).
14. Wu, B. *et al.* Structural basis for dsRNA recognition, filament formation, and antiviral signal activation by MDA5. *Cell* **152**, 276–289 (2013).
15. Rice, G. *et al.* Heterozygous mutations in *TREX1* cause familial chilblain lupus and dominant Aicardi-Goutières syndrome. *Am. J. Hum. Genet.* **80**, 811–815 (2007).
16. Tojo, K. *et al.* Dystonia, mental deterioration, and dyschromatosis symmetrica hereditaria in a family with *ADAR1* mutation. *Mov. Disord.* **21**, 1510–1513 (2006).
17. Livingston, J.H. *et al.* A type I interferon signature identifies bilateral striatal necrosis due to mutations in *ADAR1*. *J. Med. Genet.* **51**, 76–82 (2014).
18. Kondo, T. *et al.* Dyschromatosis symmetrica hereditaria associated with neurological disorders. *J. Dermatol.* **35**, 662–666 (2008).
19. Bennett, L. *et al.* Interferon and granulopoiesis signatures in systemic lupus erythematosus blood. *J. Exp. Med.* **197**, 711–723 (2003).
20. Baechler, E.C. *et al.* Interferon-inducible gene expression signature in peripheral blood cells of patients with severe lupus. *Proc. Natl. Acad. Sci. USA* **100**, 2610–2615 (2003).
21. Cen, H. *et al.* Association of *IFIH1* rs1990760 polymorphism with susceptibility to autoimmune diseases: a meta-analysis. *Autoimmunity* **46**, 455–462 (2013).
22. Crampton, S.P., Deane, J.A., Feigenbaum, L. & Bolland, S. *Ifih1* gene dose effect reveals MDA5-mediated chronic type I IFN gene signature, viral resistance, and accelerated autoimmunity. *J. Immunol.* **188**, 1451–1459 (2012).
23. Nejentsev, S. *et al.* Rare variants of *IFIH1*, a gene implicated in antiviral responses, protect against type 1 diabetes. *Science* **324**, 387–389 (2009).
24. Crow, Y.J. & Rehwinkel, J. Aicardi-Goutières syndrome and related phenotypes: linking nucleic acid metabolism with autoimmunity. *Hum. Mol. Genet.* **18**, R130–R136 (2009).
25. Stetson, D.B. Endogenous retroelements and autoimmune disease. *Curr. Opin. Immunol.* **24**, 692–697 (2012).
26. Deddouche, S. *et al.* Identification of an LGP2-associated MDA5 agonist in picornavirus-infected cells. *eLife* **3**, e01535 (2014).
27. Funabiki, M. *et al.* Autoimmune disorders associated with gain of function of the intracellular sensor MDA5. *Immunity* **40**, 199–212 (2014).
28. Crow, Y.J. *et al.* Therapies in Aicardi-Goutières syndrome. *Clin. Exp. Immunol.* **175**, 1–8 (2014).
29. Herries, D.G. *Enzyme Structure and Mechanism* 2nd edn. (W H Freeman, New York, 1985).

[1]Manchester Academic Health Science Centre, University of Manchester, Genetic Medicine, Manchester, UK. [2]Department of Biological Chemistry and Molecular Pharmacology, Harvard Medical School, Boston, Massachusetts, USA. [3]Department of Medicine, Boston Children's Hospital, Boston, Massachusetts, USA. [4]Child Neurology and Psychiatry Unit, C. Mondino National Neurological Institute, Pavia, Italy. [5]Department of Brain and Behavioral Sciences, Unit of Child Neurology and Psychiatry, University of Pavia, Pavia, Italy. [6]Department of Pediatric Immunology and Rheumatology, INSERM U768, Imagine Foundation, Assistance Publique–Hôpitaux de Paris (AP-HP), Hôpital Necker, Paris, France. [7]Department of Paediatric Rheumatology, Alder Hey Children's National Health Service (NHS) Foundation Trust, Liverpool, UK. [8]Department of Developmental Neuroscience, Istituto di Ricovero e Cura a Carattere Scientifico (IRCCS) Stella Maris, Pisa, Italy. [9]Institute of Translational Medicine, University of Liverpool, Liverpool, UK. [10]Service de Pédiatrie 1, Centre Hospitalier Universitaire (CHU) de Dijon, Dijon, France. [11]Department of Pediatrics, Azienda Ospedaliero Universitaria (AOU) Meyer and University of Florence, Florence, Italy. [12]Division of Pediatric Neurology, Department of Pediatrics, University of Colorado School of Medicine, Denver, Colorado, USA. [13]Department of Paediatrics, Rainbow House NHS Ayrshire and Arran, Irvine, UK. [14]Neuroimmunology Group, Children's Hospital at Westmead, University of Sydney, Sydney, New South Wales, Australia. [15]Department of Paediatric Rheumatology, Royal Hospital for Sick Children, Glasgow, UK. [16]Department of Paediatric Neurology, University Hospitals Leuven, Leuven, Belgium. [17]Department of Pediatric Neurology, INSERM U768, Imagine Foundation, AP-HP, Hôpital Necker, Paris, France. [18]Centre de Génétique, Hôpital d'Enfants, CHU de Dijon and Université de Bourgogne, Dijon, France. [19]Child Neurology and Psychiatry Unit. Civil Hospital, Department of Clinical and Experimental Sciences, University of Brescia, Brescia, Italy. [20]Service de Génétique Médicale, CHU de Nantes, Nantes, France. [21]INSERM, UMRS 957, Nantes, France. [22]Division of General Pediatrics, Department of Pediatrics, McMaster Children's Hospital, McMaster University, Hamilton, Ontario, Canada. [23]Université et Faculté de Medecine Paris Descartes, Paris, France. [24]Department of Pediatrics, Clinical Genetics Program, McMaster Children's Hospital, McMaster University, Hamilton, Ontario, Canada. [25]Department of Paediatric Neurology, Leeds Teaching Hospitals NHS Trust, Leeds, UK. [26]Clinics Hospital of Ribeirao Preto, University of São Paulo, São Paulo, Brazil. [27]Operative Unit Child Neuropsychiatry, Department of Neuroscience, Giannina Gaslini Institute, Genoa, Italy. [28]Institute of Infection, Immunity and Inflammation, University of Glasgow, Glasgow, UK. [29]Institute for Neuroscience and Muscle Research, Children's Hospital at Westmead, University of Sydney, Sydney, New South Wales, Australia. [30]Department of Genetics, Groupe Hospitalier Pitié Salpêtrière, AP-HP, Paris, France. [31]Paediatric Rheumatology, Giannina Gaslini Institute, Genoa, Italy. [32]Clinical Department of Pediatrics, San Paolo Hospital, University of Milan, Milan, Italy. [33]Department of Neurology, Great Ormond Street Hospital for Children, London, UK. [34]Service de Neuropédiatrie, Centre de Référence de Neurogénétique, Hôpital A. Trousseau, AP-HP, Hôpitaux Universitaire Est Parisien (HUEP), Paris, France. [35]Université Pierre et Marie Curie (UPMC), Université Paris 06, Paris, France. [36]INSERM U676, Paris, France. [37]Department of Paediatric Rheumatology, University of Cape Town, Red Cross War Memorial Children's Hospital, Cape Town, Republic of South Africa. [38]Department of Clinical Genetics, Southern General Hospital, Glasgow, UK. [39]Department of Pediatric Neurology, Children's National Medical Center, Washington, DC, USA. [40]Service de Néonatalogie et Réanimation, Hôpital Charles Nicolle, CHU Rouen, Rouen, France. [41]Neurology Department. Hospital Dona Estefânia, Centro Hospitalar de Lisboa Central, Lisbon, Portugal. [42]Division of Pediatric Neurology, Department of Pediatrics, McMaster Children's Hospital, McMaster University, Hamilton, Ontario, Canada. [43]US National Institutes of Health Undiagnosed Diseases Program, Common Fund, Office of the Director, US National Institutes of Health, Bethesda, Maryland, USA. [44]Paediatric Neurosciences Research Group, Fraser of Allander Neurosciences Unit, Royal Hospital for Sick Children, Glasgow, UK. [45]School of Medicine, College of Medical, Veterinary and Life Sciences, University of Glasgow, Glasgow, UK. [46]These authors contributed equally to this work. [47]These authors jointly directed this work. Correspondence should be addressed to Y.J.C. (yanickcrow@mac.com) or S.H. (sun.hur@childrens.harvard.edu).

ONLINE METHODS

Affected individuals and families. All affected individuals included in this study either had a clinical and neuroradiological diagnosis of AGS associated with upregulation of cerebrospinal fluid interferon and/or ISGs in peripheral blood (an interferon signature) or a neuroimmunological phenotype in the presence of an interferon signature in peripheral blood recorded in the absence of any obvious infection. Clinical information and samples were obtained with informed consent. The study was approved by the Leeds (East) Research Ethics Committee (reference number 10/H1307/132).

Exome sequencing. Genomic DNA was extracted from lymphocytes from affected individuals and their parents by standard techniques. For whole-exome analysis, targeted enrichment and sequencing were performed on 3 μg of DNA extracted from the peripheral blood of three individuals (F102, F163 and F259). Enrichment was undertaken using the SureSelect Human All Exon kits following the manufacturer's protocol (Agilent Technologies), and samples were paired-end sequenced on either an Illumina HiSeq 2000 or SOLiD platform. Sequence data were mapped using BWA (Burrows-Wheeler Aligner) using the hg18 (NCBI36) human genome as a reference. Variants were called using SOAPsnp and SOAPindel (from the Short Oligonucleotide Analysis Package) with medium stringency (**Supplementary Table 1**).

Sanger sequencing. Primers were designed to amplify the coding exons of *IFIH1* (**Supplementary Table 7**). Purified PCR amplification products were sequenced using BigDye Terminator chemistry and an ABI 3130 DNA sequencer. Mutation description is based on the reference cDNA sequence NM_022168.3, with nucleotide numbering beginning from the first A in the initiating ATG codon.

Gene expression analysis. Total RNA was extracted from whole blood using a PAXgene (PreAnalytix) RNA isolation kit. RNA concentration was assessed using a spectrophotometer (FLUOstar Omega, Labtech). qPCR analysis was performed using TaqMan Universal PCR Master Mix (Applied Biosystems) and cDNA derived from 40 ng of total RNA. The relative abundance of target transcripts, measured using TaqMan probes for *IFI27* (Hs01086370_m1), *IFI44L* (Hs00199115_m1), *IFIT1* (Hs00356631_g1), *ISG15* (Hs00192713_m1), *RSAD2* (Hs01057264_m1) and *SIGLEC1* (Hs00988063_m1), was normalized to the expression levels of *HPRT1* (Hs03929096_g1) and 18S RNA (Hs999999001_s1) and assessed with Applied Biosystems StepOne Software v2.1 and DataAssist Software v.3.01. For each of the six probes, individual (case and control) data were expressed relative to a single calibrator (control C25). As previously described, the median fold change in expression of the 6 ISGs, when compared to the median expression for the 29 healthy controls combined, was used to create an interferon score for each case[9]. The RQ value is equal to $2^{-\Delta\Delta Ct}$ (i.e., normalized fold change relative to a control). When a subject was assayed on more than one occasion, the data for repeat measurements were combined to calculate a mean value (using Applied Biosystems DataAssist software v.3.01).

Statistics. In the absence of a normal distribution, ISG levels and interferon scores were log transformed and analyzed using parametric testing (one-way ANOVA). Bonferroni or Dunnett's multiple-comparison tests were applied as detailed in **Figure 2** and **Supplementary Figure 4**. Interferon scores for each group were expressed as the median (IQR). Statistics were calculated using GraphPad Prism version 5.0d for Mac OS X.

Microsatellite genotyping. To confirm maternity and paternity, informative polymorphic microsatellite markers on chromosomes 3 (D3S3640 and D3S3560), 11 (D11S4205, D11S913, D11S987 and D11S1889) and 20 (D20S847, D20S896 and D20S843) were genotyped using DNA from F102, F524_2, F647, F626, F237, F163 and respective parents, as well as from an unrelated control sample. DNA samples were amplified by standard PCR (primer sequences available upon request). Each amplicon was mixed with HiDi Formamide (Applied Biosystems) and 500 ROX Size Standard (Applied Biosystems) and run on the Genetic Analyzer 3010 capillary electrophoresis system. Results were analyzed with GeneMapper v4.1 software (Applied Biosystems).

Protein modeling. The IFIH1 substitutions p.Arg337Gly, p.Asp393Val, p.Gly495Arg, p.Arg720Gln, p.Arg779His and p.Arg779Cys all fell within the helicase domain of the protein. Molecular graphics figures were generated with PyMOL (Schrodinger) using the PDB coordinates (4GL2).

Interferon reporter assays. The pFLAG-CMV4 plasmid encoding IFIH1 has been described elsewhere[12]. The indicated mutations were introduced using KAPA HiFi DNA polymerase. HEK 293T cells (American Type Culture Collection, ATCC) were maintained in 24-well plates in DMEM (Cellgro) supplemented with 10% heat-inactivated FCS and 1% penicillin-streptomycin. Cells were tested for mycoplasma. At ~95% confluence, cells were cotransfected with pFLAG-CMV4 plasmids encoding wild-type or mutant IFIH1 (5 ng, unless mentioned otherwise), IFN-β promoter–driven firefly luciferase reporter plasmid (200 ng) and a constitutively expressed *Renilla* luciferase reporter plasmid (pRL-CMV; 20 ng) using Lipofectamine 2000 (Life Technologies) according to the manufacturer's protocol. Medium was changed 6 h after transfection, and cells were subsequently stimulated with poly I:C (0.5 μg/ml; Invivogen) or with *in vitro*–transcribed 162-bp dsRNA (0.5 μg/ml) using Lipofectamine 2000. Cells were lysed 24 h after stimulation, and IFN-β promoter activity was measured using the Dual-Luciferase Reporter assay (Promega) and a Synergy2 plate reader (BioTek). Firefly luciferase activity was normalized against *Renilla* luciferase activity. Error bars represent s.d. from three independent experiments. For protein blot analysis, primary antibodies to Flag (F7425, Sigma-Aldrich; 1:1,000 dilution) and actin (A5441, Sigma-Aldrich; 1:1,000 dilution) were used together with horseradish peroxidase (HRP)-conjugated secondary antibodies to rabbit IgG (sc-2004, Santa Cruz Biotechnology) and mouse IgG (sc-358917, Santa Cruz Biotechnology), respectively.

Protein and RNA preparation. Wild-type IFIH1Δ2CARD and variants were expressed from pET50 (Novagen) as a 6× His–tagged NusA fusion protein in BL21(DE3) as previously described for wild-type IFIH1 (ref. 12). Briefly, cells were lysed by Emulsiflex, and proteins were purified by a combination of nickel-NTA (nitrilotriacetic acid) affinity, heparin affinity and size-exclusion chromatography in buffer A (20 mM HEPES, pH 7.5, 150 mM NaCl and 2 mM DTT). The NusA tag was removed from all proteins by human rhinovirus (HRV) 3C cleavage. Sequences for the 162-bp and 112-bp dsRNAs were taken from the first 150 and 100 nucleotides of the *IFIH1* gene, respectively, flanked by 5′-GGGAGA-3′ and 5′-TCTCCC-3′. dsRNA was prepared as previously described[12]. Briefly, two complementary strands of dsRNA were cotranscribed using T7 RNA polymerase, and duplex RNA was separated from individual strands by 8–10% PAGE followed by electroelution. The 3′ end of purified 112-bp dsRNA was subsequently labeled with fluorescein hydrazide as previously described[14].

Electrophoretic mobility shift assays and ATP hydrolysis assays. Assays were performed as previously reported[12]. Briefly, 3′ fluorescein–labeled 112-bp (20 nM) dsRNA[14] was incubated with protein (40–160 nM) in buffer B (20 mM HEPES, pH 7.5, 150 mM NaCl, 1.5 mM $MgCl_2$ and 2 mM DTT) in the presence or absence of 2 mM ATP, and complexes were analyzed on Bis-Tris NativePAGE (Life Technologies). Fluorescent gel images were recorded using the FLA9000 scanner and were analyzed with Multigauge (GE Healthcare). Curve fitting was performed using the KaleidaGraph program (Synergy). For ATP hydrolysis assays, IFIH1 (0.3 μM) was incubated with ATP (2 mM) and 112-bp dsRNA (0.6 μM) in buffer B at 37 °C. Use of an excess amount of 112-bp dsRNA (0.6 μM corresponds to 4.8 μM IFIH1-binding sites, as each 112-bp dsRNA molecule can accommodate 8 IFIH1 molecules) simplified the comparison of wild-type and mutant IFIH1 by focusing on intrinsic ATP hydrolysis activities, independent of dsRNA binding[12]. Reactions were quenched at 0 min and 5 min with 50 mM EDTA, and the levels of released phosphate were measured using GreenReagent (Enzo Lifescience) at optical density 600 (OD_{600}).

doi:10.1038/ng.2933